Acta Mech. Sin. (2012) 28(2):359–366
DOI 10.1007/s10409-012-0008-8

RESEARCH PAPER

Asymptotic analysis of outwardly propagating spherical flames

Yun-Chao Wu · Zheng Chen

Received: 22 August 2011 / Revised: 30 October 2011/ Accepted: 1 December 2011
©The Chinese Society of Theoretical and Applied Mechanics and Springer-Verlag Berlin Heidelberg 2012

Abstract Asymptotic analysis is conducted for outwardly propagating spherical flames with large activation energy. The spherical flame structure consists of the preheat zone, reaction zone, and equilibrium zone. Analytical solutions are separately obtained in these three zones and then asymptotically matched. In the asymptotic analysis, we derive a correlation describing the spherical flame temperature and propagation speed changing with the flame radius. This correlation is compared with previous results derived in the limit of infinite value of activation energy. Based on this correlation, the properties of spherical flame propagation are investigated and the effects of Lewis number on spherical flame propagation speed and extinction stretch rate are assessed. Moreover, the accuracy and performance of different models used in the spherical flame method are examined. It is found that in order to get accurate laminar flame speed and Markstein length, non-linear models should be used.

Keywords Propagating spherical flames · Asymptotic analysis · Lewis number · Stretch rate

1 Introduction

The outwardly propagating spherical flame method is currently most favorable for measuring the laminar flame speed and Markstein length [1–10]. Recently, it has been found that the laminar flame speed and Markstein length measured by this method depend strongly on the theoretical models used in the data processing [11]. These theoretical models are derived from spherical flame theory.

In the literature, outwardly propagating spherical flames have been extensively studied theoretically [12]. However, most of the theoretical studies were based on the assumption of large flame radius [12]. In spherical flame experiments measuring the laminar flame speed and Markstein length, the flame front history with large flame radii can not be used in the data processing due to the development of flame front instability [13] and/or the pressure rise [14]. Therefore, theory based on the assumption of large flame radius can not be used to derive models for data processing in spherical flame experiments [11, 12]. Only the recent work by He [15] and Chen and Ju [16] spanned all the spherical flame sizes and transitions between flames at small radii and large radii. Unfortunately, in these studies [15, 16] the propagating spherical flame is analyzed in the limit of infinite value of activation energy, while the practical hydrocarbon/air flame has finite value, large activation energy. As will be shown in this study, the results in Refs. [15, 16] are quantitatively correct when the Lewis number is close to unity and only qualitatively reasonable when the Lewis number is appreciably different from unity.

To the authors' knowledge, in the literature there is no detailed asymptotic analysis of propagating spherical flames without assuming large flame radius. Therefore the objective of this study is to present asymptotic theory on propagating spherical flames, from which different theoretical models will be derived for spherical flame experiments measuring the laminar flame speed and Markstein length. In the following, the mathematical model and asymptotic analysis are presented. Then, based on the asymptotic theory, the properties of spherical flame propagation are investigated and the models for data processing in spherical flame experiments are discussed. Finally, the conclusions are presented.

2 Mathematical model

One-dimensional, adiabatic, premixed, propagating spherical flame is analyzed using the large activation energy

The project was supported by the National Natural Science Foundation of China (50976003, 51136005) and Doctoral Fund of Ministry of Education of China (20100001120003).

Y.-C. Wu · Z. Chen (✉)
State Key Laboratory for Turbulence and Complex Systems,
Department of Mechanics and Aerospace Engineering,
Department of Aeronautics and Astronautics,
College of Engineering, Peking University,
100871 Beijing, China
e-mail: cz@pku.edu.cn

asymptotic method [17–19]. The diffusive thermal model neglecting thermal expansion (i.e. constant density) [15-20] is employed here. By assuming constant thermal and transport properties, the conservation equations for energy and fuel mass fraction are

$$\rho C_p \frac{\partial T}{\partial t} = \frac{\lambda}{r^2}\frac{\partial}{\partial r}\left(r^2 \frac{\partial T}{\partial r}\right) + q\omega,$$
$$\rho \frac{\partial Y}{\partial t} = \frac{\rho D}{r^2}\frac{\partial}{\partial r}\left(r^2 \frac{\partial Y}{\partial r}\right) - \omega, \tag{1}$$

where t, r, ρ, T and Y are time, radial coordinate, density, temperature, and fuel mass fraction, respectively. C_p is the specific heat capacity at constant pressure, λ is the thermal conductivity, q is the chemical heat-release per unit mass of fuel, and D is the mass diffusivity of fuel. Since the constant density model neglects thermal expansion, there is no convective flux in the governing equations. Moreover, the fuel lean case is studied so that only the mass fraction of fuel is considered [15–20]. The reaction rate for a one-step, irreversible, global reaction is

$$\omega = \rho A Y \exp(-E_\mathrm{a}/R^0 T), \tag{2}$$

in which A is the pre-factor of the Arrhenius law, E_a is the activation energy, and R^0 is the universal gas constant.

To simplify the analysis, we study the propagating spherical flame in the coordinate (τ, ξ) attached to the moving flame front $r = R(t)$ [15, 16]. In the new coordinate $(\tau = t, \xi = r - R(t))$, the flame can be considered as in a quasi-steady state $(\partial/\partial\tau = 0)$. This quasi-steady assumption has been widely used in previous studies [15–17, 20–23] and validated by transient numerical simulation [16]. As a result, the governing equations are simplified to

$$-\rho C_p U \frac{\mathrm{d}T}{\mathrm{d}\xi} = \frac{\lambda}{(\xi+R)^2}\frac{\mathrm{d}}{\mathrm{d}\xi}\left[(\xi+R)^2\frac{\mathrm{d}T}{\mathrm{d}\xi}\right] + q\omega, \tag{3a}$$

$$-\rho U \frac{\mathrm{d}Y}{\mathrm{d}\xi} = \frac{\rho D}{(\xi+R)^2}\frac{\mathrm{d}}{\mathrm{d}\xi}\left[(\xi+R)^2\frac{\mathrm{d}Y}{\mathrm{d}\xi}\right] - \omega, \tag{3b}$$

where $U = \mathrm{d}R(t)/\mathrm{d}t$ is the flame propagation speed.

The boundary conditions are

$$\xi = -R, \quad \mathrm{d}T/\mathrm{d}\xi = 0, \quad \mathrm{d}Y/\mathrm{d}\xi = 0, \tag{4a}$$

$$\xi \to \infty, \quad T = T_u, \quad Y = Y_u, \tag{4b}$$

where T_u and Y_u denote the temperature and fuel mass fraction in the fresh mixture, respectively.

3 Asymptotic analysis

The flame structure is shown in Fig. 1. The upstream preheat zone and downstream equilibrium zone are connected by a thin reaction zone. The asymptotic analysis is based on the concept of large activation energy [17–19]. For large activation energy, the ratio between the thickness of the inner reaction zone and that of the outer preheat/equilibrium zone is a small parameter, ε, which for the time being is unspecified but will be systematically identified later as the inverse of the Zel'dovich number [19]. The asymptotic solution will therefore be sought in ascending powers of this small parameter. Following the procedure for the asymptotic analysis of a planar flame [19], solutions will be separately obtained in these three zones constituting the flame structure and then asymptotically matched.

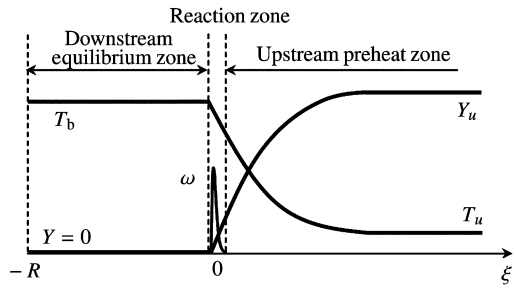

Fig. 1 The schematic flame structure

3.1 Upstream preheat zone ($\xi > 0$)

In the preheat zone, the reaction term can be neglected due to the low temperature and high activation energy. By using the boundary condition equation (4b), the asymptotic solutions in this outer zone can be obtained as

$$T^+(\xi) = T_u + C_1 \int_{R+\xi}^{\infty} s^{-2}\,\mathrm{e}^{-Us/\alpha}\,\mathrm{d}s + \varepsilon C_2 \int_{R+\xi}^{\infty} s^{-2}\,\mathrm{e}^{-Us/\alpha}\,\mathrm{d}s + O(\varepsilon^2), \tag{5a}$$

$$Y^+(\xi) = Y_u + C_3 \int_{R+\xi}^{\infty} s^{-2}\,\mathrm{e}^{-Us/D}\,\mathrm{d}s + \varepsilon C_4 \int_{R+\xi}^{\infty} s^{-2}\,\mathrm{e}^{-Us/D}\,\mathrm{d}s + O(\varepsilon^2), \tag{5b}$$

where C_i $(i = 1, 2, 3, 4)$ are integration constants to be determined through matching with the inner solution in the reaction zone and $\alpha = \lambda/(\rho C_\mathrm{p})$ is the thermal diffusivity.

3.2 Downstream equilibrium zone ($-R \le \xi < 0$)

Since the fuel is completely consumed in the reaction zone, the reaction rate becomes zero in the downstream equilibrium. The solutions in the downstream equilibrium zone are

$$T^-(\xi) = T_\mathrm{b}, \quad Y^-(\xi) = 0, \tag{6}$$

where T_b is the temperature of burned gas to be determined later (see Eq. (14)).

3.3 Matching conditions

Due to the large activation energy, the inner reaction zone is much thinner than the preheat zone and equilibrium zone.

In order to adequately resolve the reaction zone, the spatial coordinate is stretched by introducing coordinate transform: $X = \xi/\varepsilon$ [17, 19]. In the inner reaction zone, the asymptotic solutions are assumed to be

$$\begin{aligned} T_{\rm in}(X) &= \theta_0 - \varepsilon\theta_1(X) + O(\varepsilon^2), \\ Y_{\rm in}(X) &= \phi_0 + \varepsilon\phi_1(X) + O(\varepsilon^2), \end{aligned} \tag{7}$$

where θ_0 and ϕ_0 are the leading-order solutions, while $\theta_1(X)$ and $\phi_1(X)$ are perturbation functions. The solutions in the inner reaction zone will be solved in the next subsection. It is noted that the boundary condition equation (4) can not be used for solutions in the inner reaction zone. This is due to the fact that, unlike the outer preheat and equilibrium zones, the inner reaction zone is not in contact with either the upstream or the downstream boundaries. In order to determine the solutions in the inner reaction zone, matching conditions between the inner and outer solutions should be used.

The matching conditions for the inner and outer solutions at the downstream boundary of the reaction zone (i.e. $X = \xi/\varepsilon \to -\infty$) are

$$\begin{aligned} \lim_{X\to-\infty} T_{\rm in}(X) &= \lim_{X\to-\infty} T^-(X), \\ \lim_{X\to-\infty} Y_{\rm in}(X) &= \lim_{X\to-\infty} Y^-(X), \\ \lim_{X\to-\infty} {\rm d}T_{\rm in}/{\rm d}X &= \lim_{X\to-\infty} {\rm d}T^-/{\rm d}X, \\ \lim_{X\to-\infty} {\rm d}Y_{\rm in}/{\rm d}X &= \lim_{X\to-\infty} {\rm d}Y^-/{\rm d}X, \end{aligned} \tag{8}$$

Substituting Eqs. (6) and (7) into Eq. (8) yields

$$\theta_0 - T_{\rm b} = \phi_0 = 0, \tag{9a}$$

$$\theta_1(-\infty) = \phi_1(-\infty) = 0, \tag{9b}$$

$$d\theta_1(-\infty)/dX = d\phi_1(-\infty)/dX = 0. \tag{9c}$$

Similarly, using the matching conditions for the inner and outer solutions at the upstream boundary of the reaction zone (i.e. $X = \xi/\varepsilon \to +\infty$), we have

$$C_1 = (T_{\rm b} - T_u)/\int_R^\infty s^{-2}\,{\rm e}^{-Us/\alpha}\,{\rm d}\,s, \tag{10a}$$

$$C_3 = -Y_u/\int_R^\infty s^{-2}\,{\rm e}^{-Us/D}\,{\rm d}\,s, \tag{10b}$$

$$\theta_1(+\infty) \to +\infty, \tag{10c}$$

$$\phi_1(+\infty) \to +\infty, \tag{10d}$$

$$\frac{{\rm d}\theta_1(+\infty)}{{\rm d}X} = \frac{(T_{\rm b} - T_u)R^{-2}\,{\rm e}^{-UR/\alpha}}{\int_R^\infty s^{-2}\,{\rm e}^{-Us/\alpha}\,{\rm d}\,s}, \tag{10e}$$

$$\frac{{\rm d}\phi_1(+\infty)}{{\rm d}X} = \frac{Y_u R^{-2}\,{\rm e}^{-UR/D}}{\int_R^\infty s^{-2}\,{\rm e}^{-Us/D}\,{\rm d}\,s}. \tag{10f}$$

3.4 Inner reaction zone

The leading-order solutions, $\theta_0 = T_{\rm b}$ and $\phi_0 = 0$, are readily obtained through matching (see Eq. (9a)). However, the inner solutions, $\theta_1(X)$ and $\phi_1(X)$, are still unknown and they will be solved in the following. Substituting Eq. (7) and the coordinate transform $X = \xi/\varepsilon$ into Eq. (3), we can show that the convective term is one order smaller than the diffusion term and thus can be neglected. Therefore, the inner reaction zone is governed by the following reaction-diffusion equations

$$\lambda\frac{{\rm d}^2\theta_1}{{\rm d}X^2} = \varepsilon q\omega, \tag{11a}$$

$$\rho D\frac{{\rm d}^2\phi_1}{{\rm d}X^2} = \varepsilon\omega, \tag{11b}$$

in which the reaction term becomes

$$\omega = \rho A\varepsilon\phi_1 \exp(-E_{\rm a}/R^0 T_{\rm in}). \tag{12}$$

After eliminating the reaction term using Eq. (11) and using the boundary conditions at $X \to -\infty$ in Eqs. (9b) and (9c), we have

$$(\lambda/q)\theta_1 = \rho D\phi_1. \tag{13}$$

Substituting Eqs. (10e) and (10f) into the derivative form of Eq. (13) yields the following expression for the flame temperature

$$T_{\rm b} = T_u + \frac{qY_u}{C_{\rm p}}\frac{1}{Le}\,{\rm e}^{\frac{UR}{\alpha}(1-Le)}\frac{\int_R^\infty s^{-2}\,{\rm e}^{-Us/\alpha}\,{\rm d}\,s}{\int_R^\infty s^{-2}\,{\rm e}^{-Us/D}\,{\rm d}\,s}, \tag{14}$$

where $Le = \alpha/D$ is the Lewis number. It is seen that $T_{\rm b}$ is equal to the adiabatic flame temperature of unstretched planar flame $T_{\rm ad} = T_u + qY_u/C_{\rm p}$ when $Le = \alpha/D = 1$. Substituting Eqs. (13) and (12) into Eq. (11a) and using the boundary conditions at $X \to -\infty$ in Eqs. (9b) and (9c) and $X \to +\infty$ in Eqs. (10c) and (10e), we have

$$\frac{R^{-2}\,{\rm e}^{-UR/\alpha}}{\int_R^\infty s^{-2}\,{\rm e}^{-Us/\alpha}\,{\rm d}\,s} = \sqrt{\frac{2}{Z^2}\frac{A}{D}\exp\left(-\frac{E_{\rm a}}{R^0 T_{\rm b}}\right)}. \tag{15}$$

Therefore, from the above asymptotic analysis, the flame temperature, $T_{\rm b}$, and flame propagation speed, U, can be determined as functions of flame radius, R, by Eqs. (14) and (15).

In the limit of zero flame propagation speed ($U = 0$), Eqs. (14) and (15) are reduced to the results for the flame temperature and radius of stationary flame ball [24, 25]. Therefore, the flame ball solution is a limiting case of the present result. Moreover, in the limit of infinite flame radius ($R \to \infty$), Eqs. (14) and (15) are reduced to solutions for adiabatic planar flames. Therefore, the present theory is valid for spherical flames with small and large radii.

4 Results and discussions

By solving Eqs. (14) and (15) numerically, the relation between the flame propagation speed U and flame radius R can be obtained and thus the properties of propagating spherical flame can be investigated.

4.1 Asymptotic results in the non-dimensional form

To get general conclusions, the asymptotic results are first transformed into non-dimensional form. By using adiabatic planar flame speed $S_L = \{2\alpha Le Z_{ad}^{-2} A \cdot \exp[-E_a/(R^0 T_{ad})]\}^{1/2}$ [18, 19] and the planar flame thickness $\delta_f^0 = \alpha/S_L$ as the characteristic speed and length scale, respectively, the flame propagation speed, flame radius, and flame temperature can be normalized as

$$U' = \frac{U}{S_L}, \quad R' = \frac{R}{\delta_f^0}, \quad T_b' = \frac{T_b - T_u}{T_{ad} - T_u}. \tag{16}$$

It is noted that the Zel'dovich number, $Z_{ad} = E_a(T_{ad} - T_u)/(R^0 T_{ad}^2)$, is based on the adiabatic planar flame temperature, $T_{ad} = T_u + qY_u/C_p$, which is different from T_b for propagating spherical flames when $Le \neq 1$ (see Eq. (14)).

By substituting Eq. (16) into Eqs. (14) and (15), the following relationships for the non-dimensional flame temperature and flame propagation speed as functions of flame radius can be obtained (after dropping the primes)

$$T_b \frac{R^{-2}\,\mathrm{e}^{-UR}}{\int_R^\infty s^{-2}\,\mathrm{e}^{-Us}\,\mathrm{d}s} = \frac{1}{Le}\frac{R^{-2}\,\mathrm{e}^{-ULeR}}{\int_R^\infty s^{-2}\,\mathrm{e}^{-ULes}\,\mathrm{d}s} = [\sigma + (1-\sigma)T_b]^2 \exp\left[\frac{Z_{ad}}{2}\frac{T_b - 1}{\sigma + (1-\sigma)T_b}\right], \tag{17}$$

where σ is the ratio between the temperature of the fresh mixture and the adiabatic planar flame temperature. It is noted that in the following the non-dimensional flame temperature (T_b), flame propagation speed (U), and flame radius (R) are presented without the primes.

4.2 Comparison with previous studies

In the recent studies of Refs. [15, 16], the propagating spherical flame is analyzed in the limit of infinite value of activation energy, $E_a \to \infty$, and the chemical reaction rate is assumed to be a Delta function. The following relationships are obtained for adiabatic propagating spherical flames [15, 16]

$$T_b \frac{R^{-2}\,\mathrm{e}^{-UR}}{\int_R^\infty s^{-2}\,\mathrm{e}^{-Us}\,\mathrm{d}s} = \frac{1}{Le}\frac{R^{-2}\,\mathrm{e}^{-ULeR}}{\int_R^\infty s^{-2}\,\mathrm{e}^{-ULes}\,\mathrm{d}s} = \exp\left[\frac{Z_{ad}}{2}\frac{T_b - 1}{\sigma + (1-\sigma)T_b}\right]. \tag{18}$$

Comparison between Eqs. (17) and (18) shows that the only difference is the factor before the exponential term. In fact, in Refs. [15, 16], the Zel'dovich number should be defined as $Z = E_a(T_{ad} - T_u)/(R^0 T_b^2)$ which is not constant since the flame temperature changes with flame radius for $Le \neq 1$. Equation (18) holds only when the flame temperature is close to the adiabatic planar flame (i.e. $T_b \approx 1$) so that $[\sigma + (1-\sigma)T_b]^2 \approx 1$.

Figure 2 shows the change of the non-dimensional flame temperature and flame propagation speed with the flame radius at different Lewis numbers. The Zel'dovich number, $Z_{ad} = 10$, and the thermal expansion ratio, $\sigma = 0.15$, are fixed for all the theoretical results except those in Figs. 3 and 6. The present asymptotic results (Eq. (17)) are compared with those in Refs. [15, 16] (Eq. (18)). For $Le = 1$, the non-dimensional flame temperature is independent of the flame radius ($T_b \equiv 1.0$ for $Le = 1$ according to Eq. (17)). Therefore, the factor before the exponential term in Eq. (17) is always equal to 1.0, which indicates that Eqs. (17) and (18) give the same result. However, for non-unity Lewis number, the non-dimensional flame temperature is different from unity at finite flame radius ($T_b \neq 1.0$). Therefore, as shown in Fig. 2, the results predicted by Eq. (17) are different from those by Eq. (18) when $Le \neq 1$. When the Lewis number is close to unity ($Le = 0.8$ or 1.2) or the flame radius is large enough ($R > 100$), the spherical flame temperature is close

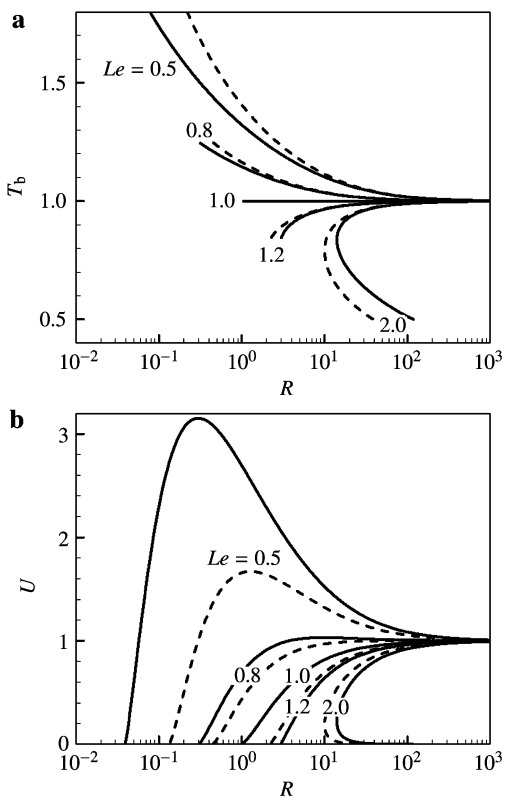

Fig. 2 Change of the **a** flame temperature and **b** flame propagation speed with the flame radius. Solid lines: results predicted by Eq. (17); dashed lines: results predicted by Eq. (18)

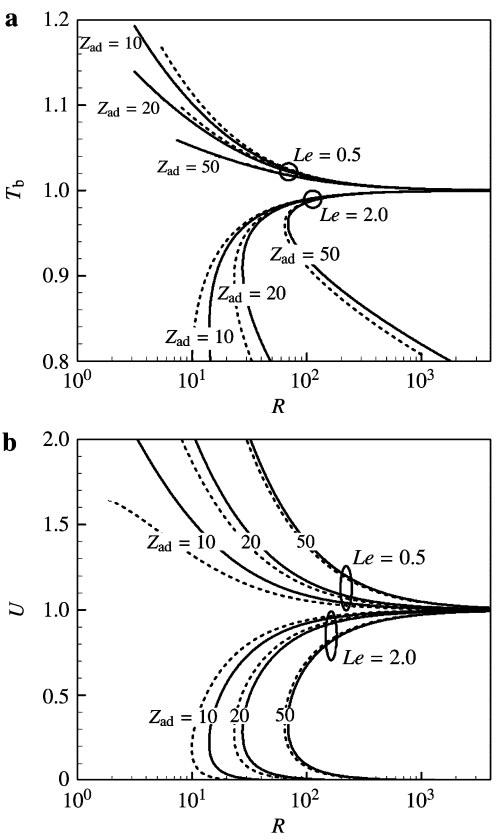

Fig. 3 Effects of the Zel'dovich number on the prediction of the **a** flame temperature and **b** flame propagation speed given by different formula. Solid lines: results predicted by Eq. (17); dashed lines: results predicted by Eq. (18)

to the planar flame temperature (see Fig. 2a), which makes the factor, $[\sigma + (1-\sigma)T_b]^2$, close to unity. As a result, Fig. 2 shows that the predication by Eq. (17) is close to that by Eq. (18) when the Lewis number is close to 1.0 ($Le = 0.8$ or 1.2) or the flame radius is large ($R > 100$). However, when the Lewis number is apparently different from unity ($Le = 0.5$ or 2.0) and the flame radius is small ($R < 100$), the results predicted by these two equations are quite different.

Equation (17) is obtained by the large activation energy asymptotic method while Eq. (18) is derived using the delta function model assuming infinite value of activation energy. So it is supposed that the prediction by Eq. (17) should tend to that by Eq. (18) with increasing Zel'dovich numbers. This is demonstrated by Fig. 3 which presents results at different Zel'dovich numbers (Z_{ad} = 10, 20, and 50). As expected, Fig. 3 shows that the larger the Zel'dovich number (activation energy), the smaller the difference between the results predicted by Eqs. (17) and (18).

For the combustion of most of the hydrocarbon fuels, the Zel'dovich number is in the range of 5.0–15.0. Therefore, the results obtained in the limit of infinite value of activation energy (the chemical reaction rate is assumed to be a Delta function) in Refs. [15, 16], i.e. Eq. (18), are quantitatively correct only when the Lewis number is close to unity and only qualitatively reasonable when the Lewis number is appreciably different from unity. Consequently, the present asymptotic results, Eq. (17), should be used, especially for Lewis number apparently different from unity and for small flame radius. In the following, all the results are obtained from Eq. (17).

4.3 Properties of propagating spherical flames

The change of the flame propagation speed with the stretch rate is shown in Fig. 4. For outwardly propagating spherical flames, the non-dimensional stretch rate is defined as

$$K = \frac{1}{A}\frac{\mathrm{d}A}{\mathrm{d}t} = \frac{2}{R}\frac{\mathrm{d}R}{\mathrm{d}t} = \frac{2U}{R}, \tag{19}$$

where $A = 4\pi R^2$ is the non-dimensional surface area of the spherical flame.

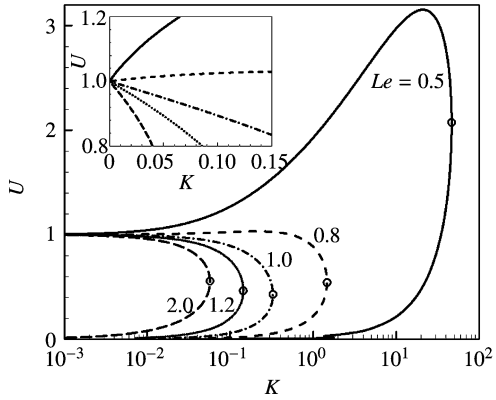

Fig. 4 Change of the flame propagation speed with the stretch rate

As shown in Fig. 4, the Lewis number strongly affects the change of U with K. This is caused by the coupling between the positive stretch rate and preferential thermal-mass diffusion [16, 19, 22]. The inset in Fig. 4 shows that at small stretch rate, the flame propagation speed varies almost linearly with the stretch rate. The spherical flame method is based on this linear behavior such that the unstretched laminar flame speed and Markstein length can be obtained from the linear extrapolation of U and K [2, 3, 5–9].

Figure 4 further shows that for each Lewis number, there exists a maximum stretch rate (denoted by circle in the figure) beyond which no propagating spherical flame exists. This maximum stretch rate is defined as the extinction stretch rate, K_{ext}. Spherical flame propagation occurs only when the stretch rate is smaller than the extinction stretch rate. Similar definition was also used by Bradley et al. [26] in their study on the extinction stretch rate of premixed ethanol/air flames. The change of the extinction stretch rate with the Lewis number is shown in Fig. 5. It is seen that the extinction

stretch rate decreases exponentially with the Lewis number. This is due to the fact that the smaller the Lewis number, the more strongly the spherical flame is enhanced by its positive stretch rate [16, 19, 22] and hence the more difficult it is extinguished. Similar conclusion was drawn in the analysis of premixed counterflow flames [27–29].

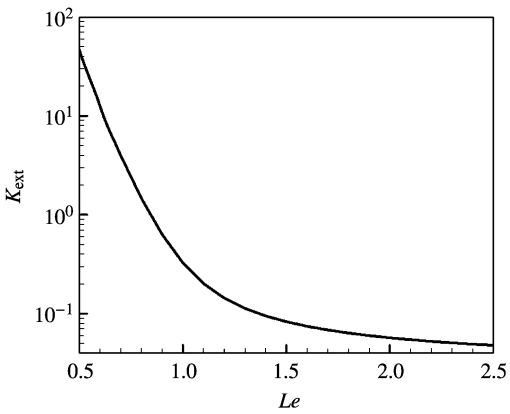

Fig. 5 The extinction stretch rate as a function of Lewis number

4.4 Different models for the spherical flame method

Recently, it has been found that the laminar flame speed and Markstein length measured by the spherical flame method [1–9] depend strongly on the theoretical models used in the data processing [11]. In Ref. [11], one linear model (LM, the stretched flame speed changes linearly with the stretch rate) and two non-linear models (NM-I and NM-II, the stretched flame speed changes non-linearly with the stretch rate) were derived from the detailed model (DM) given by Eq. (18). Similarly, the following LM, NM-I, and NM-II can also be derived from the DM given by Eq. (17)

$$U = 1-2L^0U/R, \quad U = 1-2L^0/R, \quad \ln(U) = -2L^0/(RU), \tag{20}$$

where the normalized Markstein length L^0 (normalized by the planar flame thickness, δ_f^0) is given by

$$L^0 = \frac{1}{Le} - \left[2(1-\sigma) + \frac{Z_{ad}}{2}\right]\left(\frac{1}{Le} - 1\right). \tag{21}$$

The form of these three models (LM, NM-I, and NM-II) derived from Eq. (17) is the same as those from Eq. (18) in Ref. [11]. However, according to Eq. (21), the normalized Markstein length depends on not only Le and Z_{ad}, but also σ. Figure 6 presents the change of the normalized Markstein length with the Lewis number. As expected, the Markstein length increases monotonically with the Lewis number. Moreover, Fig. 6 shows that the influence of the temperature ratio, σ, on the Markstein length is nearly negligible compared to that of the Zel'dovich number, Z_{ad}.

Similar to our recent study [11], the accuracy of the LM, NM-I, and NM-II given by Eq. (20) can be assessed by comparison with DM given by Eq. (17). The results are presented in Fig. 7. It is seen that the predictions by the LM, NM-I, and NM-II converge to that by the DM when the non-dimensional stretch rate is small enough (or the flame radius is large enough). For $Le = 1$, the predictions by the LM, NM-I, and NM-II are shown to be close to that by the DM in

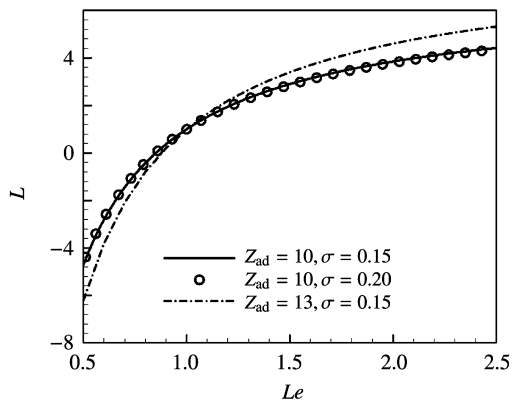

Fig. 6 Change of the normalized Markstein length with the Lewis number

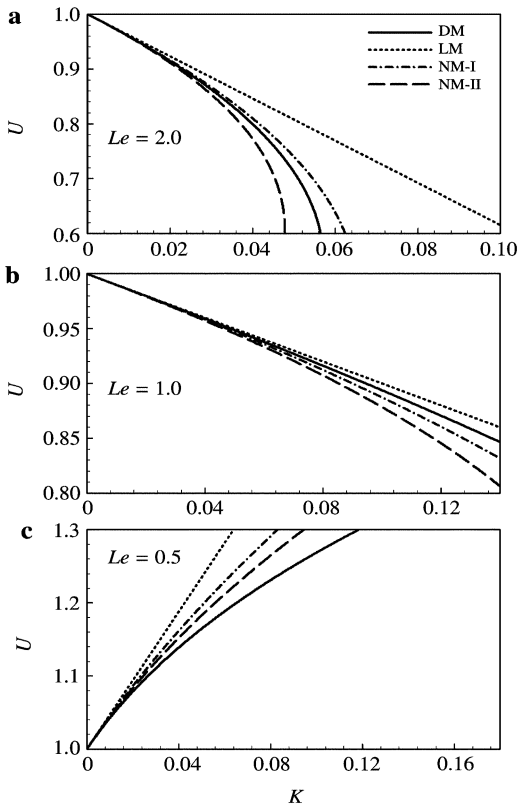

Fig. 7 Flame propagation speed as a function of the stretch rate predicted by different models

the whole range of stretch rate considered, while for $Le = 2.0$ and 0.5, there is very large difference between the predictions by the LM, NM-I, and NM-II and that by the DM, especially at large stretch rate. This is because when the Lewis number is appreciably different from unity, the relative difference between the stretched and unstretched flame speeds will be greater than 20% (i.e. $|U - 1| > 0.2$) for large stretch rate, as shown in Figs. 7a and 7c. As a result, the assumption of $|U - 1| = |\varepsilon| \ll 1$ used to derive the LM, NM-I, and NM-II is not strictly satisfied [11]. Moreover, Fig. 7 shows that the accuracy of NM-I and NM-II depends on the Lewis number: NM I is closer to the DM than NM II for $Le = 2.0$, while NM II is closer to the DM than NM I for $Le = 0.5$. The same conclusion was drawn in Ref. [11] based on the results given by Eq. (18) instead of Eq. (17).

In order to demonstrate the performance of these models in extracting the laminar flame speed and Markstein length in the spherical flame method, the extracted and exact unstretched flame speeds, U^0, and Markstein lengths, L, are compared in Fig. 8. The data utilized for extraction are exact results from the DM given by Eq. (17) at $R = 20, 25 \ldots, 100$. It is seen that the relative difference between extracted and exact values for U^0 is within 20%, while that for L can be above 200%. Moreover, the performance of the LM, NM-I, and NM-II is seen to strongly depend on the Lewis number. For mixtures with Lewis number appreciably different from unity, both the laminar flame speed and the Markstein length are over-predicted from extractions based on the LM. Therefore, in order to get accurate laminar flame speed and Markstein length from the spherical flame method, non-linear models should be used. Figure 8 shows that NM I is the most accurate for mixtures with large Lewis number (positive Markstein length) while NM-II is the most accurate for mixtures with small Lewis number (negative Markstein length). Again, the same conclusion was drawn in Ref. [11] based on the results given by Eq. (18) instead of Eq. (17). Therefore, the conclusion on the different models made in Ref. [11] (based on Eq. (18) obtained in the limit of infinite value of activation energy in Refs. [15, 16]) is correct.

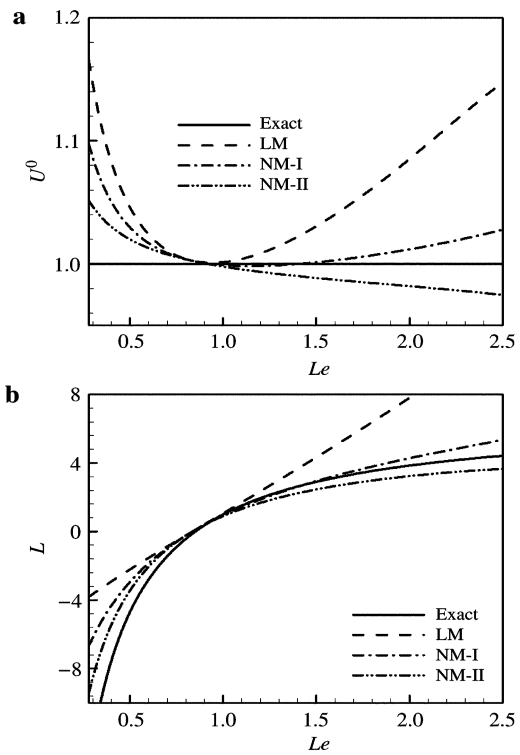

Fig. 8 Exact and extracted **a** flame speeds and **b** Markstein lengths from different models

5 Conclusions

We conduct asymptotic analysis on outwardly propagating spherical flames with large activation energy. Correlations describing the spherical flame temperature and propagation speed are derived as functions of the flame radius. These correlations are compared with previous results derived in the limit of infinite value of activation energy. It is shown that the results obtained in the limit of infinite value of activation energy are only qualitatively reasonable when the Lewis number is appreciably different from unity. Based on the correlation derived in this study, the properties of spherical flame propagation are investigated. The extinction stretch rate is found to decrease exponentially with the Lewis number. Moreover, the accuracy and performance of three different models, LM, NM-I, and NM-II, used in the spherical flame method are examined. It is found that in order to get accurate laminar flame speed and Markstein length from the spherical flame method, non-linear models should be used. The same conclusion was drawn in Ref. [11] based on results obtained in the limit of infinite value of activation energy, and thus the conclusion on the different models made in Ref. [11] is proven correct.

References

1 Taylor, S.C.: Burning velocity and the influence of flame stretch. [Ph.D. Thesis], University of Leeds (1991)

2 Tseng, L.K., Ismail, M.A., Faeth, G.M.: Laminar burning velocities and Markstein numbers of hydrocarbon/air flames. Combust. Flame **95**, 410–426 (1993)

3 Bradley, D., Hicks, R.A., Lawes, M., et al.: The measurement of laminar burning velocities and Markstein numbers for iso-octane-air and iso-octane-n-heptane-air mixtures at elevated temperatures and pressures in an explosion bomb. Combust Flame **115**, 126–144 (1998)

4 Tse, S.D., Zhu, D.L., Law, C.K.: Morphology and burning rates of expanding spherical flames in H_2/O_2/inert mixtures up to 60 atmospheres. Proc. Combust. Inst. **28**, 1793–1800 (2000)

5 Qin, X., Ju, Y.: Measurements of burning velocities of dimethyl ether and air premixed flames at elevated pressures. Proc.

Combust. Inst. **30**, 233–240 (2005)

6 Huang, Z., Zhang, Y., Zeng, K., et al.: Measurements of laminar burning velocities for natural gas-hydrogen-air mixtures. Combust. Flame **146**, 302–311 (2006)

7 Chen, Z., Qin, X., Ju, Y.G., et al.: High temperature ignition and combustion enhancement by dimethyl ether addition to methane-air mixtures. Proc. Combust. Inst. **31**, 1215–1222 (2007)

8 Hu, E., Huang, Z., He, J., et al.: Experimental and numerical study on laminar burning characteristics of premixed methane-hydrogen-air flames. Int. J. Hydrogen Energy **34**, 4876–4888 (2009)

9 Qiao, L., Gan, Y., Nishiie, T., et al.: Extinction of premixed methane/air flames in microgravity by diluents: Effects of radiation and Lewis number. Combust. Flame **157**, 1446–1455 (2010)

10 Tang, C.L., Huang, Z.H., Law, C.K.: Determination correlation and mechanistic interpretation of effects of hydrogen addition on laminar flame speeds of hydrocarbon-air mixtures. Proc. Combust. Inst. **33**, 921–928 (2011)

11 Chen, Z.: On the extraction of laminar flame speed and Markstein length from outwardly propagating spherical flames. Combust. Flame **158**, 291–300 (2011)

12 Chen, Z., Burke, M.P., Ju, Y.: Effects of Lewis number and ignition energy on the determination of laminar flame speed using propagating spherical flames. Proc. Combust. Inst. **32**, 1253–1260 (2009)

13 Bradley, D., Lawes, M., Liu, K., et al.: Laminar burning velocities of lean hydrogen-air mixtures at pressures up to 1.0 MPa. Combust. Flame **149**, 162–172 (2007)

14 Chen, Z., Burke, M.P., Ju, Y.: Effects of compression and stretch on the determination of laminar flame speed using propagating spherical flames. Combust. Theor. Model. **13**, 343–364 (2009)

15 He, L.T.: Critical conditions for spherical flame initiation in mixtures with high lewis numbers. Combust. Theor. Model. **4**, 159–172 (2000)

16 Chen, Z., Ju, Y.: Theoretical analysis of the evolution from ignition kernel to flame ball and planar flame. Combust. Theor. Model. **11**, 427–453 (2007)

17 Buckmaster, J.D., Lundford, G.S.S.: Theory of Laminar Flames. Cambridge University Press (1982)

18 Williams, F.A.: Combustion Theory (2nd edn). Benjamin-Cummins, Menlo Park, California USA (1985)

19 Law, C.K.: Combustion Physics. Cambridge University Press (2006)

20 Frankel, M.L., Sivashinsky, G.I.: On quenching of curved flames. Combust. Sci. Technol. **40**, 257–268 (1984)

21 Frankel, M.L., Sivashinsky, G.I.: On effects due to thermal-expansion and Lewis number in spherical flame propagation. Combust. Sci. Technol. **31**, 131–138 (1983)

22 Chen, Z., Gou, X., Ju, Y.: Studies on the outwardly and inwardly propagating spherical flames with radiative loss. Combust. Sci. Technol. **182**, 124–142 (2010)

23 Zhang, H., Chen, Z.: Spherical flame initiation and propagation with thermally sensitive intermediate kinetics. Combust. Flame **158**, 1520–1531 (2011)

24 Zeldovich, Y.B., Barenblatt, G.I., Librovich, V.B., et al.: The Mathematical Theory of Combustion and Explosions. New York: Consultants Bureau (1985)

25 Champion, M., Deshaies, B., Joulin, G., et al.: Spherical flame initiation theory versus experiments for lean propane-air mixtures. Combust. Flame **65**, 319–337 (1986)

26 Bradley, D., Lawes, M., Mansour, M.S.: Explosion bomb measurements of ethanol–air laminar gaseous flame characteristics at pressures up to 1.4 MPa. Combust. Flame **156**, 1462–1470 (2009)

27 Ju, Y., Guo, H.S., Liu, F.S., et al.: Effects of the Lewis number and radiative heat loss on the bifurcation and extinction of $CH_4/O_2/N_2/He$ flames. J. Fluid Mech. **379**, 165–190 (1999)

28 Ju, Y., Masuya, G., Liu, F., et al.: Asymptotic analysis of radiation extinction of stretched premixed flames. Int. J. Heat Mass Tran. **43**, 231–239 (2000)

29 Chen, Z., Ju, Y.: Combined effects of curvature, radiation, and stretch on the extinction of premixed tubular flames. Int. J. Heat Mass Tran. **51**, 6118–6125 (2008)